

Analysis of Magneto-inductive System for Rocket Sled Velocity Measurement Beyond Mach 1.5

P.K. Khosla*, Rajesh Khanna¹, and Sanjay P. Sood[§]

**Terminal Ballistics Research Laboratory, Chandigarh -160003, India*

¹Thapar Institute of Engineering and Technology, Patiala -147004, India

[§]Centre for Development of Advanced Computing, Mohali - 160071, India

**E-mail: pkk7@yahoo.com*

ABSTRACT

The rail track rocket sled (RTRS) national test facility at Terminal Ballistics Research Laboratory (TBRL) has been established to provide simulated flight environment for carrying out aero dynamic studies, terminal studies and kinematic studies of variety of test articles. The sled velocity is a critical parameter in evaluation trials. This velocity is also used to ensure that the maximum speed and allowable g loading does not exceed the value which the test article will experience under free flight in air¹. Overseas, the facilities have been set up to attain velocities ranging from sub-sonic to hypersonic². The rocket sled at TBRL can be presently accelerated to travel along the rail track at velocities up to 500 m/s and capability is being built to increase velocity beyond 500 m/s. Signals acquired from existing magneto-inductive arrangement have been analysed in the present work. The experiments indicate that with increase in velocity the rate of change of flux increases, the amplitude of induced emf also increases but terminal voltage decreases and shape of the acquired pulse gets distorted. The parameters of magneto-inductive pick up have been modified in such a way that there is improvement in amplitude and shape of the received pulse with increase in velocity. The improved signals have been analysed and simulation results validated with feasible experiments. This paper also discusses issues, challenges and proposes recommendations in improving the sensor for measurement of velocity beyond Mach 1.5. It has been found that it is prudent to reduce the inductance by reducing the number of turns and changing the core from soft iron core to air core which will improve the response of inductive pick up coil at high velocity.

Keywords: Magneto-inductive, sensor, sled velocity, supersonic velocity, rail track, rocket sled, magneto-kinematic

1. INTRODUCTION

The problem of the motion of a magnetic field due to the motion of a permanent magnet has been subject of scientific controversy for many decades^{3,4}. The debate has been whether the field due to permanent magnet exhibits wave like behaviour or moves as a body. It has bearing on our understanding of the way emf is induced. The discussion goes on from old papers⁷⁻⁹ to the current papers^{3,4}. The present work is not a work on this theory but being experimental outcome of a practical application wherein simple modifications enhance the capability and will help studies in magneto-kinematics, too.

The pickup coil sensors are one of the oldest and operating principles of coil sensor are generally known, but technical details and practical implementation of induction coil sensor are only known to specialists⁵. The implementation of magneto-inductive technology in an application specific integrated circuit (ASIC) which gives inherently digital output (oscillates) and resolution of the order of 10 nT can be obtained while sensing external magnetic field⁶ and are commercially available. The disadvantage of such a system is that it does not offer a time reference, requires a board to be designed along with ASIC, driver and multiplex circuit. Further, 1200 such boards with power supply need to be deployed in the field. The

proposed sensor is just a pickup coil which is ruggedized for use in field.

At RTRS the test articles are mounted on specially designed sleds, which slides and accelerates down the rail track, to the desired velocity using solid propellant rocket motors. The sled velocity is a critical parameter in all dynamic trials. At RTRS, the measurement of sled velocity at regular distances is carried out through a magnet and coil system. As shown in Fig 1, a U-shaped (or horse-shoe) magnet is mounted on the sled and inductive pickups are fixed along the rail track at 10 m separation from one another. Although use of inductive pickups for measurement of sled velocity was reported more than 50 years ago^{7,8}, but even now the interest in these systems continues to grow. This is mainly because of the fact that the network of magneto-inductive sensors can be installed over distances of several kilometres and yet they obtain large signals without any excitation or signal conditioning and the sensor can be fabricated by user. Use of accelerometers in combination with coils has also been reported⁹, which are forgotten but are relevant in the present context. A feasibility study to measure velocity using interferometry¹⁰ has been carried out but no further development has been reported. In this study the signal pulse from network of magnet and coil



Figure 1. Deployment of sensor along the track.

arrangement has to propagate distances as large as 4 km. The sensor is passive, that is, there is no excitation or active circuit and the arrangement is maintenance-free. The moving magnet, generates an approximately sinusoidal voltage signal in the pickup coil which is transmitted through a coaxial cable to record the corresponding ‘instantaneous’ event time in the data acquisition system. The sled velocity is computed from such recorded event intervals and the known separation distance between the fixed coils. The study will help the readers understand the limitations of pickup and how to improve it so as to capture faster phenomenon.

1.1 Problems Faced Due to Limitations of Existing Approaches

The existing magnet-coil velocity measurement system, installed nearly 25 years ago, has served the intended purpose, its overall precision and consistency needs to be significantly improved to meet the current and futuristic challenges but with some shortcomings. The present analysis of the existing velocity measurement system has been undertaken with the objective of improving its detection beyond Mach 1.5 and to remove the known shortcomings. The major challenges which still need to be addressed are:

- Significant attenuation in signal at higher sled velocities. The attenuation is so high that the signal will not be detectable at higher velocities, beyond Mach 1.5. The signal will further attenuate when more coils will be added in parallel due to doubling of the length of rail track under the augmentation programme.
- Distortion in the signal pulse shape tends to increase with increasing sled velocity.
- Problems in estimating the instantaneous sled velocity from distorted pulse shape due to shifting of reference point.

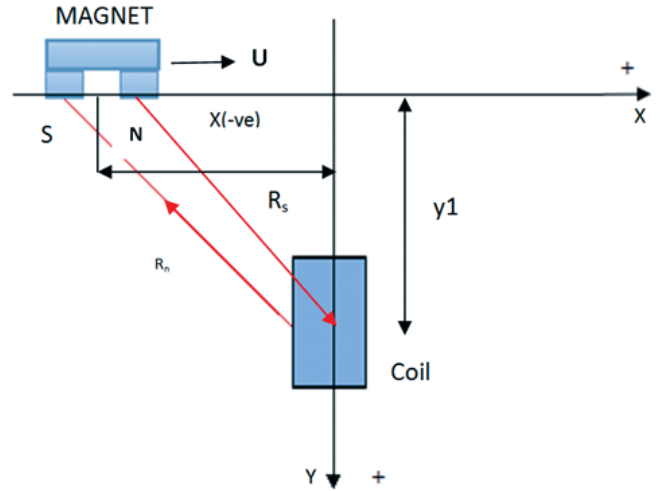


Figure 2. Schematic representation of magnet moving over the coil.

2. SALIENT FEATURES OF EXISTING SETUP

A schematic representation of the existing velocity measurement system is shown at Fig. 2. Each pole face of the U shaped magnet mounted on the sled is of 11.5 mm X 30 mm area. The distance (d) between the two pole faces is about 32 mm. Specified maximum magnetic field strength (B_0) of about 1500 Gauss (0.15 T) corresponds to an equivalent pole strength (p) of about 80 Am. Such an equivalent magnetic pole can be assumed to be located around 6 mm (half pole width) inside the pole face. On the basis of equivalent magnetic pole strength (+ for North and – for South pole), the effective magnetic flux density, at a distance r from the pole (along r vector), can be computed as,

$$B = \frac{\mu_0 P}{4\pi r^2} \text{ T} \tag{1}$$

where μ_0 is the permeability of free space in T.m/Amp

If R_n is the radial distance from north pole to the center of coil and R_s is the radial distance from south pole to the center of coil, with y_1 as the vertical distance of the coil center from the two poles (Fig. (3)), the downward (along Y axis) component of resultant magnetic flux density B_y due to the combined effect

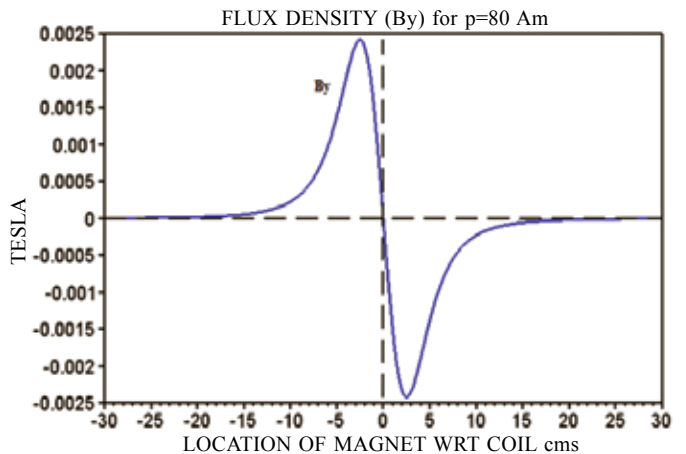


Figure 3. Variation of magnetic flux density by with relative location of magnet wrt coil.

of two poles is given by,

$$B_y = \frac{\mu_0 p y_1}{4\pi} \left(\frac{1}{(R_n)^3} - \frac{1}{(R_s)^3} \right) T \quad (2)$$

A graph of magnetic flux density, B_y (Eqn. (2)) for various positions of the magnet on the X-axis is given at Fig. 4. The variation of flux density B_y along X-axis is obviously independent of the sled velocity.

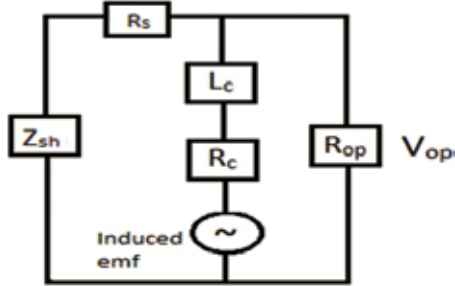


Figure 4. Equivalent circuit of the magneto-inductive velocity measurement system at RTRS.

The existing sensor coil consists of 10,000 turns (N_c) of fine copper wire (SWG-36) wound around 18 mm diameter soft iron core of 38 mm length. The ohmic resistance (R_L) of the coil is 650Ω and the inductance (L_c) of the coil is 2.5 Henry. Let A_c denote the core cross-sectional area in m^2 , then the total magnetic flux in the core will be given by $B_y A_c$ in Webers. Then

$$E = -\frac{d}{dt}(N_c B_y A_c) = -N_c A_c \frac{d}{dx}(B_y) \frac{dx}{dt} = -U N_c A_c \frac{d}{dx}(B_y) \text{ Volts} \quad (3)$$

Therefore, when the magnet moves over the fixed coil at velocity U along the X-axis, the induced emf (E) in the coil of N_c turns can be found from Eqn. (3).

2.1 Analysis of Existing Sensor

Without taking into account any marginal effects of a lossless transmission line, the pulse voltage output of the sensor coil, at the load end, can be estimated from an equivalent circuit diagram shown at Fig. 4. The impedance Z_{sh} of the other sensors in parallel and the line resistance R_s has been ignored for simplicity. Here, the magnet induced EMF (Eqn. 3) in the coil drives a current I through coil resistance R_L , coil inductance L_c and the output load resistance R_{op} . Applying Kirchhoff's voltage law for the voltage drops across various elements in the current loop, we get the following relationship.

$$E - IR_L - L_c \frac{dI}{dt} - IR_{op} = 0 ; V_{op} = E - IR_L - L_c \frac{dI}{dt} \quad (4)$$

$$\text{Or, } \frac{dI}{dt} = \frac{1}{L_c} (E - I(R_c + R_{op})) \quad (5)$$

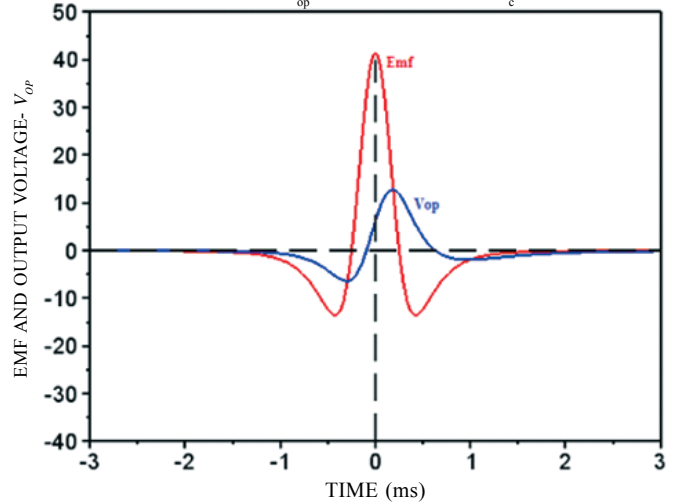
Substituting the value of E from Eqn. (3) as a function of x or t , and solving Eqn. (5) through improved Euler method of numerical integration, to obtain an I pulse corresponding to the E pulse of Eqn. (3).

The output voltage (V_{op}) pulse is then obtained through $V_{op} = IR_{op}$. The R_{op} is set $4.7 \text{ k}\Omega$ during track testing and $1.8 \text{ k}\Omega$ while testing on the rotor. The value was so chosen that the

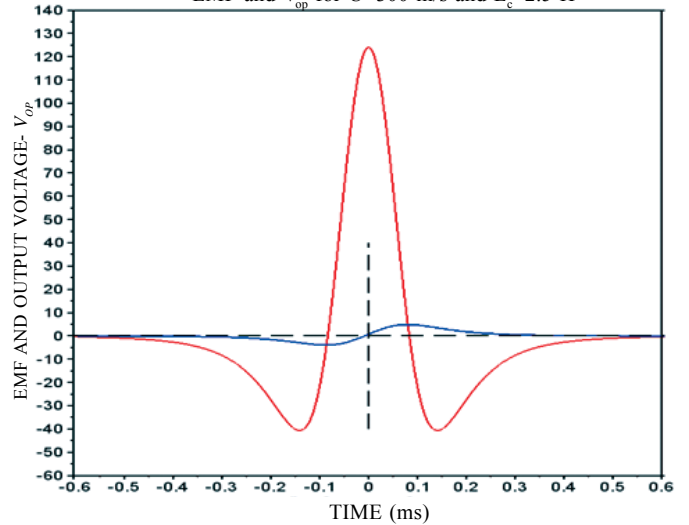
sensor output remains within $\pm 5 \text{ V}$ input range of the PC base data acquisition card.

Three sample signal pulses for E and V_{op} at velocities

EMF and V_{op} for $U=100 \text{ m/s}$ and $L_c=2.5 \text{ H}$



EMF and V_{op} for $U=300 \text{ m/s}$ and $L_c=2.5 \text{ H}$



EMF and V_{op} for $U=1000 \text{ m/s}$ and $L_c=2.5 \text{ H}$

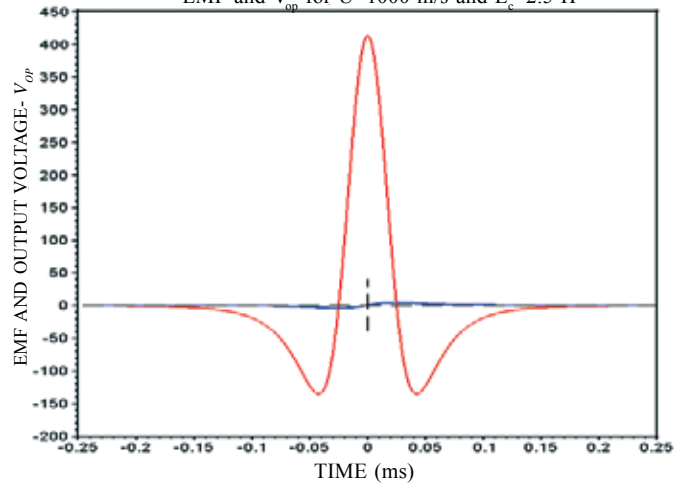


Figure 5. Variation of induced emf and the output terminal voltage with respect to magnet crossing over the magneto-inductive sensor at 100 m/s, 300 m/s and 1000 m/s velocity and with air core $L_c = 2.5 \text{ H}$.

of 100 m/s, 300 m/s, 1000 m/s obtained using SCILAB 5.4.0 application package are shown in Fig. 5.

2.2 Experiment with Existing Sensor at Highest Feasible Velocity

An experiment was conducted on rail track. The maximum velocity achieved in this experiment was 500 m/s. Presently, available infrastructure does not allow achieving velocity higher than 500 m/s on the rail track. The experiment was carried out with 20 sensors connected in parallel. Table 1 and Fig. 6 show that the value of peak amplitude reduces with velocity. The signal from existing sensor will not be detectable beyond 500 m/s. In this experiment an existing inductive pick up of 2.5 H, soft iron core was used and the signal captured shown in Fig. 7.

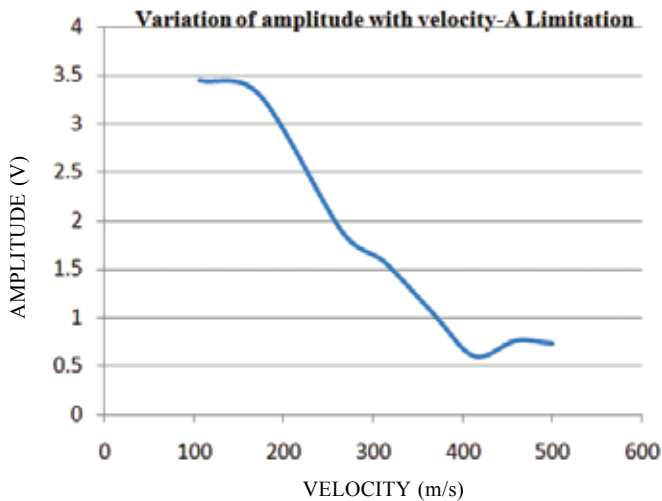


Figure 6. Experimental data with velocity up to 500 m/s.

Table 1. Experimental data of track testing with $R_{op} = 4.7 \text{ k}\Omega$.

Velocity (m/s)	Peak amplitude (V)
106	3.445
173	3.298
266	1.873
312	1.575
368	1.028
413	0.596
459	0.757
500	0.730

The distortion in terminal voltage is similar to the simulation results of Fig 5. In simulation the drop across shunted coils and transmission line is not considered as the focus is to study the attenuation of signal with velocity in the isolated sensor. The fabrication of proposed sensor will also be in small quantity as the large quantity required for parallel network of sensors cannot be realised without finalising isolated sensor. The decision for detection of signal is taken for +ve amplitude, so as to have consistent reference for pulse to pulse interval.

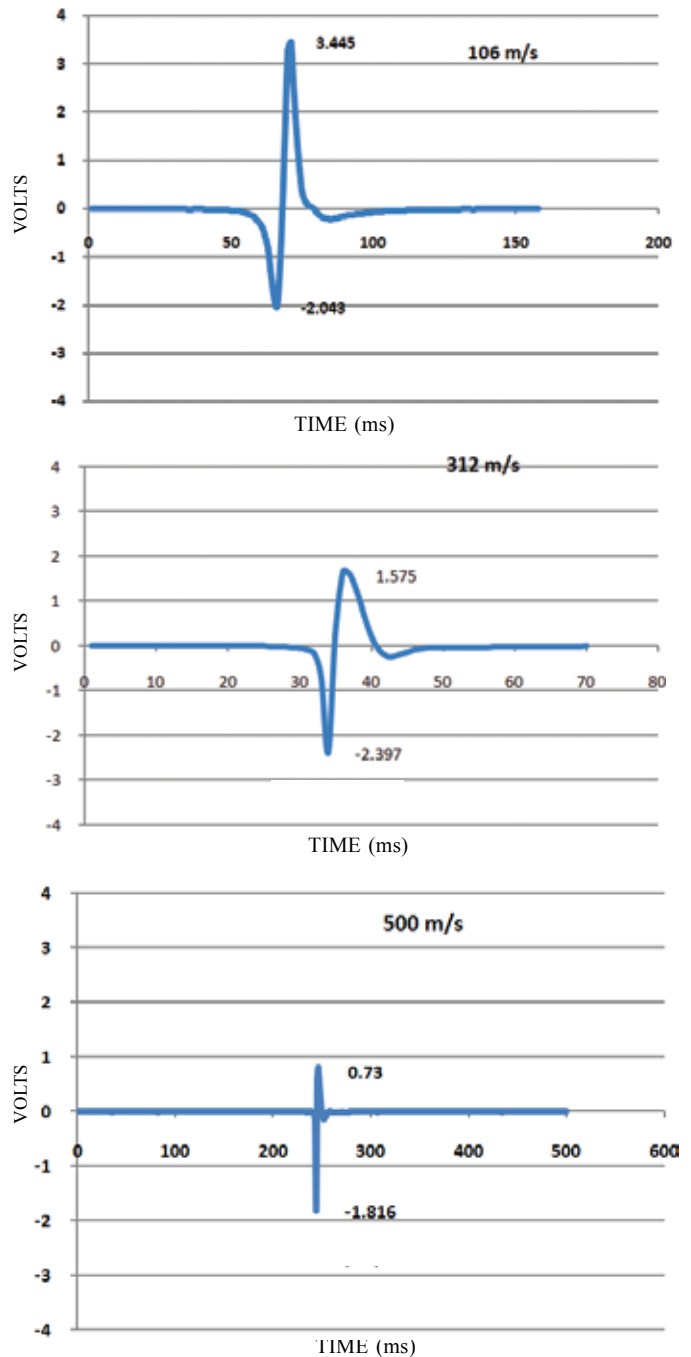


Figure 7. Signals captured at 106 m/s, 312 m/s and 500 m/s in experiment on rail track.

Further, a diode can be connected across each coil when very large number of sensors is connected in parallel. These diodes will eliminate the 2nd -ve peak. The amplitude has reduced from 3.2 V at 106 m/s to 1.5 V at 312 m/s and to 0.73 V at 500 m/s. The value at serial no 6 in Table 1 is erroneous may be due to relatively large separation between magnet and sensor.

Figure 7 show the waveform of the signals received from field sensors. Simulation results of Fig. 5 when compared with the experimental results shown at Fig. 7 shows that in existing sensor the positive peak attenuates, trailing -ve pulse gets distorted and reduces in amplitude as the velocity increases. As the focus is to study the sensor alone, simulation has not

taken into consideration the effect of transmission line and the shunting due to other sensors on the same line which were there in experiments.

3. PROPOSED CHANGES IN THE MAGNETO-INDUCTIVE SENSOR

The inductive sensors can be directly manufactured by users⁵. These are the best sensors when dimensions are not a constraint⁵. Although the focus of this paper is analysis but with minor changes the capability of the sensor to detect higher velocities gets enhanced. The Eqns. (3) and (4) show that induced emf is desirable but large L_c is undesirable. In the sensor, the output falls with increase in velocity (Fig. 6) due to high value of inductance. The inductance L_c of the sensor coil is high because of its soft iron core, which also adversely effects the high frequency response. It may be noted that the coil inductance is directly proportional to the relative permeability μ_r of the core material. However, in the present set up the magnetic flux density B linking permanent magnet and the inductive sensor is nearly independent of μ_r of the core material. Hence the provision of soft iron core in the sensor coil merely increases the value of inductance L_c without increasing the total flux or the induced emf in the coil. Therefore, it is proposed that the soft iron core be eliminated. Tumanski⁵ reports the non-linearity of coil with core can be removed by changing it to air cored sensors and gives following empirical formula for inductance.

$$L_c = N_c^2 \frac{\mu_0 \mu_c A_c}{l_c} \left(\frac{l}{l_c} \right)^{-3/5}$$

where μ_c is the resultant permeability of the core and is much lower than the permeability of the material, l and l_c are the coil and the core length respectively.

Further, if the number of turns are halved, the emf will also become $\frac{1}{2}$ as per Eqn. (3) but the inductance will reduce by $\frac{1}{4}$. An attempt was also made with turns reduced to $\frac{1}{4}$ th, but results were better when turns were reduced to $\frac{1}{2}$ in case of isolated L_c . Further, experiments and studies were done using the proposed sensor along with the existing sensor so as to have identical magnet to coil gap and velocity. The realized inductance was measured using LCR meter for coil of 10,000,

5000, 4000 and 2500 turns. Except existing coil of 10,000 turns, remaining all were air core coils.

4. COMPARISON OF IMPEDANCE OFFERED BY EXISTING AND PROPOSED SENSOR AT DIFFERENT VELOCITIES

It is the impedance which attenuates the output voltage with increase in velocity. Therefore, comparison of impedances was undertaken. The signal pulse produced in the sensor coil, is transmitted to the output load (R_{op}) of about $4.7 \times 10^3 \Omega$, through a coaxial cable of more than 2 km length. The cable used at RTRS is a twin coaxial cable (RG 58C) of characteristic impedance (Z_0) 50Ω , line capacitance 100 pf/m and line inductance of 2.4×10^{-7} H/m with a velocity factor of about 68 percent. In the kHz frequency range of the signal pulse, the coaxial cable functions as a lossless transmission line. As such a high impedance output load (R_{op}) is used in the present case for monitoring the signal pulse voltage. Consequently, a part of the signal power does get reflected from the output end of the cable. Presently the output impedance is $4.7 \times 10^3 \Omega$. It will be fully absorbed at the far end of the cable, if terminated with a matched impedance of 50Ω .

Further, in the present case it is not feasible to match the sensor coil impedance with the characteristic line impedance of the cable since the inductive reactance of the coil keeps increasing with the velocity of the rocket sled. Therefore, under the circumstances, full power of the signal pulse does not get transferred to the transmission cable. The power transfer from the induced signal pulse in the sensor coil to the coaxial cable can however be maximized by minimizing the inductive reactance of the coil by minimizing its inductance.

To calculate the impedance, nominal frequency (f_r) of the induced emf pulse can be computed from the time period of the pulse as seen in Fig. 5 above. Total impedance Z_c of the coil with inductance L_c and internal resistance R_L is given by,

$$Z_c = \sqrt{(R_L^2 + (2\pi f_r L_c)^2)} \quad (6)$$

Since frequency f_r of the pulse increases with sled velocity, total impedance of the coil will also increase with the

Table 2. Simulated studies of parameters of existing and proposed sensors

Sled velocity U (m/s)	Nominal frequency f_r (Hz)	Impedance Z_c (k Ω) of existing sensor for $L_c=2.5$ H, $R_L=650\Omega$	Impedance Z_c (k Ω) of proposed sensor for $L_c=0.284$ H, $R_L=250 \Omega$
50	5.896×10^2	9.284	1.081
100	1.179×10^3	18.531	2.118
200	2.358×10^3	37.045	4.215
300	3.538×10^3	55.578	6.318
400	4.717×10^3	74.097	8.420
500	5.896×10^3	92.616	10.523
600	7.075×10^3	111.135	12.627
700	8.255×10^3	129.670	14.732
800	9.434×10^3	148.190	16.836
900	1.061×10^4	166.662	18.934
1000	1.179×10^4	185.198	21.039

velocity. The corresponding total impedance of the coil with iron core and air core is given in Table 2 for different values of the rocket sled velocity.

4.1 Comparative Estimation of Variation of Output Voltage with Velocity

Due to the voltage drop across the coil inductance L_c the output voltage V_{op} available across load R_{op} gets reduced considerably in comparison with the induced emf. The impedances of Table 2 have been taken into consideration in calculating output. Comparison of maximum values of this output voltage for the soft iron core ($L_c = 2.5$) and for air core ($L_c = 0.284$ H) versions of the sensor coil is given in Table 3. It is observed that the voltage output from proposed sensor is higher for any given velocity. It may be noted that these values are for isolated sensors. They will become part of a network of parallel sensor during implementation and the output in that case will fall considerably. As the experimental data show that in case of existing sensor it becomes so less that the output is not detectable. In case of proposed sensor the output remains appreciably high even at higher velocities and can be detected by data acquisition card.

The sensor impedance is much more than the characteristic line impedance of the coaxial cable. Therefore, the amplitude of the output voltage is likely to get further attenuated because the full power of the induced pulse cannot get transferred to the transmission line due to the impedance mismatch. The sample signal pulses for E and V_{op} obtained for the soft iron core coil of L_c 2.5 H and air cored coil with L_c of 0.284 Henry are given below in Figure 8. As seen from these

Figures, with the decrease in coil impedance, the output voltage approaches the induced emf not only in amplitude but also in shape. That is, the distortion in the output voltage pulse noted with soft iron core gets minimized with the use of air core due to the corresponding reduction in coil impedance. Simulation results of variation of induced emf and the output terminal voltage with magnet crossing over the coil at 100 m/s, 300 m/s and 1000 m/s respectively using existing sensor having soft iron core are shown in Fig 5. The difference between induced emf and output voltage is more at higher velocity due to increase in impedance of coil with velocity.

5. COMPARISON OF EXPERIMENTALLY ACQUIRED SIGNALS FROM REALISED SENSORS

Since it is not viable to conduct rocket sled test on and off for validation. The experiments need to be conducted with identical magnet to sensor gap and identical velocity. To meet the requirement a rotating fan with radius 1 m was improvised (See Fig. 10). The magnets were fixed on both ends of the fan. The sensor coil was stationary and opposite the magnet. The sensor C1 is the existing sensor and C2 is the proposed sensor. Initially a velocity of the order of 36 m/s could only be achieved and results are shown in Fig. 9. The gap between magnet and coil was kept 33 mm so as to have a signal within ± 5 V range of data acquisition card of National Instruments (NI) which was used for this purpose. Table 4 lists the 3 sensors used in experiment and its comparative data. The

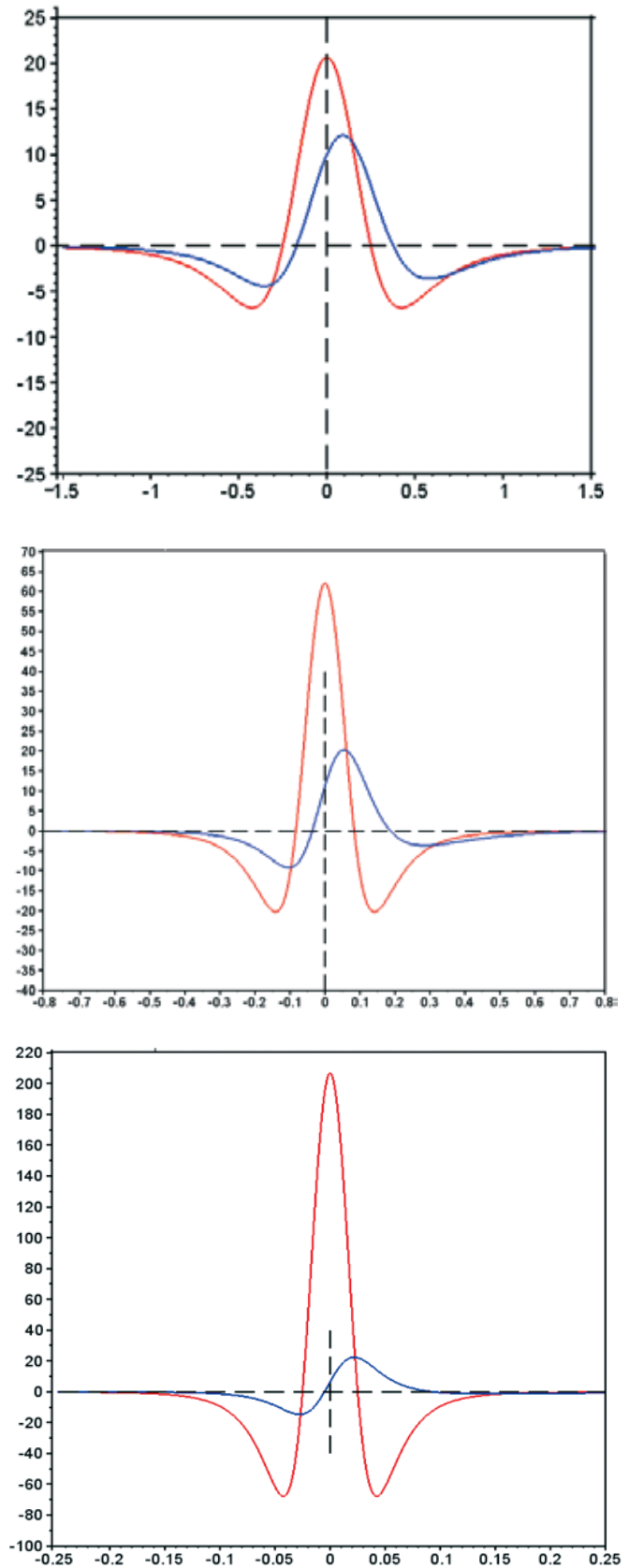


Figure 8. Variation of induced emf (in red) and the output terminal voltage (in blue) with respect to magnet crossing over the magneto-inductive sensor at velocity of 100 m/s, 300 m/s and 1000 m/s and with proposed air core sensor having $L_c = 0.284$ H.

Table 3. Simulation results of output of sensors at different velocities and identical conditions

Relative velocity	Existing sensor		Proposed sensor	
	$L_c = 2.5 \text{ H}, R_L = 650 \Omega, \text{ Turns} = 10000$ $R_{op} = 1.8 \text{ k} \Omega$		$L_c = 0.284 \text{ H}, R_L = 250 \Omega, \text{ Turns} = 5000$ $R_{op} = 1.8 \text{ k} \Omega$	
m/s	emf (volts)	V_{op} (volts)	emf (volts)	V_{op} (volts)
60	24.80	5.030	12.40	9.52
100	41.34	5.098	20.67	13.63
300	124.00	4.831	62.00	21.05
500	206.70	4.702	103.30	22.31
800	330.70	4.631	165.30	22.40
1000	410.00	4.581	206.70	22.23

Table 4. Comparison of amplitude at 36 m/s

Core	Turns		Expt 1 +ve pk (V)	Expt 2 +ve pk (V)	Expt 3 +ve pk (V)
C1: Soft Iron	10000	Set 1	3.15	3.2	3.15
		Set 2	3.72	3.66	3.76
C2: Air Core	5000	Set 1	5.0	4.9	5.0
		Set 2	5.0	5.0	5.0
C3: Air Core	2500	Set 1	3.12	3.2	3.22
		Set 2	3.27	3.16	3.24

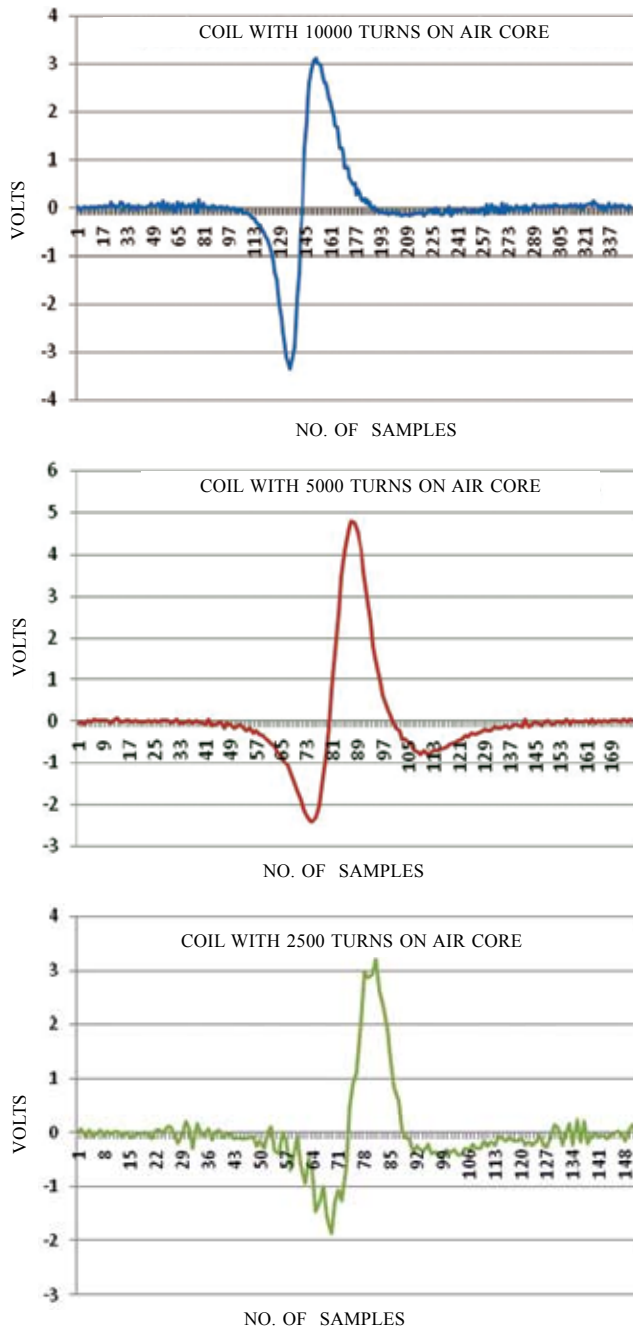


Figure 9. Experimentally acquired signals captured at 36 m/s velocity using rotor.

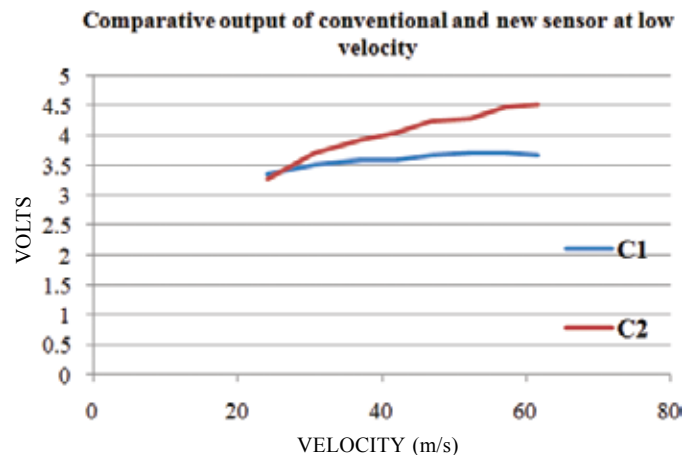


Figure 10. Rotating magnet and experimental results.

data set 1 was taken again on another day with recording as set 2 so as to have adequate data and check consistency. As per results of simulation, reducing the inductance would improve the high velocity response of the sensor. However, reducing inductance should not be so much that it reduces the amplitude below threshold at low velocity. Table 4 shows that the sensor C2 with L_c 0.284 H gives higher output and is proposed as a choice for further work involving larger quantity of sensors. Further improvements were carried out in the rotor apparatus so as to attain higher velocity and to check validation at range of velocities. The results are shown as comparison of existing and proposed sensors at different velocity when tested on rotor as shown in Table 5. Magnet to sensor gap was kept at gap of 34 mm. The gap was kept fixed as we have focused on relative performance.

Table 5. Comparative experimental data

Vel (m/s)	2.5 H	0.284 H
	C1(V)	C2(V)
24.19	3.35	3.27
30.70	3.511	3.71
37.16	3.592	3.913
42.05	3.592	4.033
47.00	3.672	4.234
52.35	3.712	4.274
57.25	3.712	4.475
61.68	3.672	4.515

The focus of study has been the comparison of amplitude and shape of the existing and proposed sensor rather than the comparison of absolute values of amplitude. It reduces the efforts in experimentation as the gap between magnet and pickup need not be changed. The load resistance in this case had to be reduced to meet the requirement of within ± 5 V range of data acquisition card. It is found that the amplitude is higher and distortion is less in case of air core based sensor with $L_c = 0.284$ H and it validates the findings of simulation results, too.

This sensor is recommended for use in establishing network of sensors along the rail track. The experiments at higher velocity will be feasible thereafter.

6. FUTURE SCOPE OF WORK

The future work includes realization of sensors in larger quantity and experimenting on the track when capability to achieve higher sled velocity is acquired. In field implementation the proposed sensor will become part of network of hundreds of other similar sensors. The effect of change in sensor impedance with velocity will have effect on coupling of signal with the transmission line. There will also be effect of loading of impedance by other sensors, especially, at lower velocity. The effect of change in reference for calculation of time will generate error and needs to be quantified. Finding the instantaneous velocity from single pulse will be a challenge and this study will be a step in that direction. These effects need to be studied and their remedy proposed.

7. CONCLUSION

It is found that 10,000 turn iron core based inductive sensor has limitation of amplitude at higher velocity. As soon as the signal level falls below the threshold level of 0.7 V at Mach 1.5, it cannot be detected due to noise in the long distance transmission lines. Moreover, the 2nd negative peak attenuates significantly thereby distorting the signal and shifting the reference. The proposed sensor is air core based with lesser inductance. It has higher output voltage for any given velocity. Unlike existing sensor, the signal can be detected for measurement of velocity beyond 500 m/s. The distortion in the signal is also considerably lower. In this process the sensor has become capable of use at higher velocities.

ACKNOWLEDGEMENT

We thank Gp Capt GS Sandhu (Retd) and Mrs Sonu Devi for their suggestions and improvements in presentation.

REFERENCES

1. Nakata, Daisuke; Yajima, Jun; Nishine, Kenji; Higashino, Kazuyuki & Tanatsugu, Nobuhiro. Research and development of high speed test track facility in Japan. *In Aerospace Exposition 09 - 12 January 2012, Nashville, Tennessee* pp.8.
2. Turnbull, Dennis; Hooser, Clinton & Hooser, Michael. Soft sled test capability at the Holloman high speed test track. *AIAA 2010-1708 U.S. Air Force T&E Days 2010 2 - 4 February 2010, Nashville, Tennessee.*
3. Leus, Vladimir & Taylor, Stephen. Experimental evidence for the magneto-kinematic effect. *In Progress in Electromagnetic Research Seminar (PIERS) Proceedings, Moscow, Russia, August 19-23, 2012.*
4. Leus, Vladimir A. Magneto-kinematical and electro-kinematical fields. *Progress In Electromagnetics Research M*, 2013, **32**, pp.27-41.
5. Tumanski, Slawomir. Induction coil sensors– a review. *Measurement Sci. Techno.*, **18** R31 doi:10.1088/0957-0233/18/3/R01.
6. Andrew, Leuzinger & Andrew, Taylor. Magneto-inductive technology overview. A white paper by PNI Sensor Corporation; www.pnicorp.com, Feb 2010.
7. Beutler, F.J. & Rauch, L.L. Precision measurement of supersonic rocket sled velocity. *J. Jet Propulsion*, 1957, **27** (9), pp.1021-1024
8. Beutler, F.J. Precision measurement of supersonic rocket sled velocity-Part II. *J. Jet Propulsion*, 1958, **28**, 809-816, doi:10.2514/8.7463
9. Stirton, J. & Glatt, B. Hybrid velocity data for the velocity measuring system of the supersonic naval ordnance research track. *In the Proceedings of the IRE*, 1959, **963**, pp.1
10. Naumann, W.; Engberg, K.; Hogg, R.D.; Hunka, J. & Oliver, G. Rocket sled improved velocity measuring system feasibility study. Defense Technical Information Center, 1980.

CONTRIBUTORS



recipient of *DRDO Award for Performance Excellence - 2006* and *National Technology Day Award - 2012*.

Mr P.K. Khosla has passed MTech (ECE) from Kurkshetra University. He is presently working as Group Director of Rail Track Rocket Sled National Test Facility of TBRL and Group Director (Automation & Networking). His current interests include velocimetry and working on various elements to double the speed of rocket sled from present capability of Mach 1.5. He is



paper in International Journals. He has guided more than 60 ME theses and guiding 10 PhD students. His research interest includes wireless and mobile communication, and antennas.

Dr Rajesh Khanna received his ME (Electrical Communication) from Indian Institute of Science, Bangalore, in 1998 and PhD (Wireless Communications) from Thapar University, in 2006. Presently he is working as Professor in the Department of Electronics and Communication at Thapar Institute of Engineering and Technology, Patiala. He has published more than 30



research and development including academics in the domain of healthcare IT & eGovernance. He has authored over 60 articles including five book chapters on cutting edge applications of IT in healthcare.

Dr Sanjay P. Sood obtained his PhD in Information Technology. Currently, he is the Head & Principal Consultant, State eGovernance Mission (Chandigarh Administration), Chandigarh. He has been the founder Director at C-DAC School of Advanced Computing in Mauritius. He has conceptualized and lead program management, project implementations,